TETRAHEDRON-BUBBLE MINIMIZATION BY METACALIBRATION

Drew Johnson & Gary Lawlor

Abstract

The shapes made by soap films and bubbles have long been interesting candidates for perimeter and surface area minimization proofs. A breakthrough method called metacalibration promises not only to provide interesting alternate proofs for some solved problems, but to give access to some previously unsolved problems. This paper introduces this method and shows its application in the proof that the shape formed by a soap film on a tetrahedral wire frame with a bubble in the center is the minimal surface area way to connect the wire frame and enclose the volume.

1. Metacalibration

Metacalibration is a new proof method developed by the second author that promises to be an important complement to variational methods in the solution of outstanding isoperimetric problems. One such problem is the triple bubble in space, which "could take another hundred years" with purely variational methods [**6**, p 826], (see also [**2**]). A candidate function to metacalibrate the triple bubble is easy to write down, and it appears now (as of the date of submission of the present paper) that the biggest hurdle that still remained for competing the proof has been successfully passed.

The result in the present paper gives the first published example of a minimal configuration that is seemingly outside the grasp of current variational ideas, but is handled well by metacalibration. The surface we prove minimizing (see Figure 1) is, in fact, rather closely related to multiple bubble problems. Four large equal-sized bubbles clustered in the standard way form a tetrahedral cone at the cluster's center, and a fifth small bubble inserted at the center will form the shape seen in Figure 1. This configuration will be discussed in Section 2.

First, the following proposition introduces the form that metacalibration proofs take.

Proposition 1.1 (Metacalibration)**.** *Let $\bar{S}$ be the set of configurations that satisfy a given set of constraints, and let $\mathcal{P} : \bar{S} \to \mathbb{R}$ be some quantity to be minimized. Assume a subset S is dense in $\bar{S}$, in the sense that for any $\tau \in \bar{S}$ and $\epsilon > 0$, there exists $\sigma \in S$ such that $|\mathcal{P}(\sigma) - \mathcal{P}(\tau)| < \epsilon$.*

Then, given $\mu \in \bar{S}$, a conjectured minimizer of $\mathcal{P}$, μ is a minimizer if for each $\sigma \in S$ there exist continuous real valued functions $P_\sigma(t)$ and $g_\sigma(t)$ on an interval $\left[t_\sigma^0, t_\sigma^1\right]$ such that the following are satisfied:

1) $P_\sigma(t_\sigma^1) - P_\sigma(t_\sigma^0) = \mathcal{P}(\sigma)$

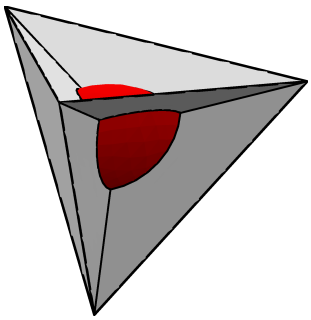

Figure 1. The tetrahedral soap complex. Image generated by Ken Brakke's Surface Evolver [**1**].

2) $g_\sigma(t_\sigma^1) - g_\sigma(t_\sigma^0) = \mathcal{P}(\mu)$.
3) g'_σ *and* P'_σ *exist except at finitely many points and are bounded.*
4) $g'_\sigma(t) \leq P'_\sigma(t)$ *whenever both derivatives exist.*

Proof. Assume for contradiction that there exists $\bar{\sigma} \in \bar{S}$ such that $\mathcal{P}(\bar{\sigma}) < \mathcal{P}(\mu)$. Then, by the density property, there exists a $\sigma \in S$ such that $\mathcal{P}(\sigma) < \mathcal{P}(\mu)$. Now, because of the hypotheses on g_σ and P_σ, the Fundamental Theorem of Calculus applies to both, and we have

$$\begin{aligned}
\mathcal{P}(\sigma) &= P_\sigma(t_\sigma^1) - P_\sigma(t_\sigma^0) \\
&= \int_{t_\sigma^0}^{t_\sigma^1} P'_\sigma(t)dt \\
&\geq \int_{t_\sigma^0}^{t_\sigma^1} g'_\sigma(t)dt \\
&= g_\sigma(t_\sigma^1) - g_\sigma(t_\sigma^0) \\
&= \mathcal{P}(\mu)
\end{aligned}$$

a contradiction. q.e.d.

The subscript σ emphasizes that the functions g and P depend on the competitor, but we will often omit them for brevity.

We say that the function g (of σ and t) metacalibrates the figure μ. The power of metacalibration lies in the fact that we create the metacalibrating function using functions that depend on properties the competitors.

The function P is often defined by slicing the figure by lines or planes, or perhaps by using arc length or other ways to measure the accumulation of the quantity to be minimized. These ideas are more easily demonstrated than explained, and we offer the following example. This isoperimetric proof, in its original form, is due to M. Gromov (see [**5**, p 120]); here we translate Gromov's proof into our metacalibration version.

Theorem 1.2. *Among all closed curves in the plane enclosing an amount of area* $\mathcal{A}$*, a circle with radius* $r = \sqrt{\frac{\mathcal{A}}{\pi}}$ *has the least perimeter.*

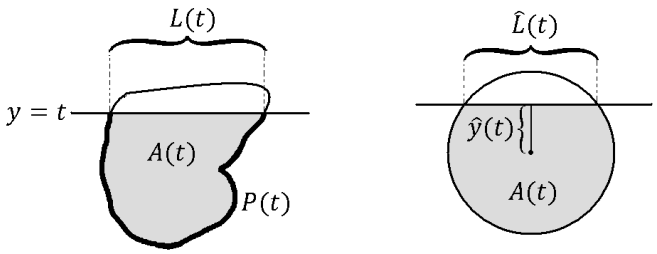

Figure 2.

Proof. $\mathcal{P}(\sigma)$ is the quantity we want to minimize, so in this case, it will the perimeter of figure σ. For any competitor σ, we will define our function P by slicing a competitor by a horizontal line $y = t$, and letting $P(t)$ be the length of the perimeter of the competitor lying beneath the slicing line. Note that by choosing a t_0 and t_1 such that $y = t_0$ is below the figure and $y = t_1$ is above it, we satisfy condition (1) of Proposition 1.1.

We will also need some other functions to help us define the metacalibrating function g. Define $L(t)$ to be the length of the intersection of the slicing line with the enclosed area, and $A(t)$ to be the amount of enclosed area beneath the slicing line.

Next, we slice the proposed minimizer, the circle, with a line so that the area under the line is equal to $A(t)$, thus matching the area under the slicing line in the competitor. Define $\hat{y}(t)$ to be the signed distance from this line to the center of the circle. Define $\hat{L}(t)$ to be the length of the intersection of this line with the circle. This is illustrated in Figure 2. The process of defining variables by matching some quantity with the proposed minimizer is an idea we will call *emulation*. Variables defined in this manner are designated with a hat (ˆ). Emulation will play an important role in the main result of this paper.

Now, we are ready to define g. For brevity of notation, we omit the parameters and subscripts, but remember that A, L, and $\hat{y}$ are functions of t and depend on the competitor. Let

$$g(t) = \frac{1}{r}\left(2A - \hat{y}L\right). \tag{1}$$

Note that $g(t_1) - g(t_0) = \frac{2\mathcal{A}}{r} = 2\sqrt{\mathcal{A}\pi}$ for any figure, since $L = 0$ for lines above and below the competitor, and since this is the perimeter of the conjectured minimizer, we have satisfied condition (2) of Proposition 1.1.

We choose our dense subset of competitors to be the set of piecewise linear closed curves which enclose the required area and which have no line segment parallel to the x-axis. It is clear that this set is dense in the sense required. Choosing this subset ensures that $A(t)$, $\hat{y}(t)$, $P(t)$, and $L(t)$ are continuous and have bounded derivatives except at finitely many points (the "corners" of the curve), thus satisfying condition (3).

Figure 3. Balancing ΔL on the left and right minimizes ΔP.

Now, we want to verify condition (4). Differentiating (1), noting that $A' = L$, we get

$$\begin{aligned} g'(t) &= \frac{1}{r}\left(2L - \hat{y}'L - \hat{y}L'\right) \\ &= \frac{1}{r}\left[\left(2 - \hat{y}'\right)L - \hat{y}L'\right]. \end{aligned}$$

Now, using the chain rule, $L(t) = A'(t) = \hat{y}'(t)\frac{d}{d\hat{y}}A(t) = \hat{y}'(t)\hat{L}(t)$. Substituting, we get

$$g'(t) = \frac{1}{r}\left[\left(2 - \hat{y}'\right)\hat{y}'\hat{L} - \hat{y}L'\right].$$

If we treat $\hat{y}'$ as an independent variable, the maximum of $\left(2 - \hat{y}'\right)\hat{y}'$ is 1, when $\hat{y}' = 1$. Hence,

$$g'(t) \leq \frac{1}{r}\left(\hat{L} - \hat{y}L'\right). \tag{2}$$

We need now to consider $P'(t)$. Take an arbitrary strip of the competitor between y and at a nearby line $y + \Delta y$, with $\Delta y > 0$ small enough that the curves in the competitor are linear. For a given ΔL, the least perimeter that slice could have is $2\sqrt{\Delta y^2 + \left(\frac{\Delta L}{2}\right)^2} = \sqrt{4\Delta y^2 + \Delta L^2}$ (see Figure 3). Dividing by Δy and taking the limit shows that

$$P'(t) \geq \sqrt{4 + L'^2}. \tag{3}$$

Now, we can rewrite (2) as a dot product and apply the Cauchy-Schwartz inequality.

$$\begin{aligned} g'(t) &\leq \frac{1}{r}\left(\hat{L} - \hat{y}L'\right) \\ &= \frac{1}{r}\left\langle \frac{\hat{L}}{2}, -\hat{y} \right\rangle \cdot \langle 2, L' \rangle \\ &\leq \frac{1}{r}\left\| \left\langle \frac{\hat{L}}{2}, -\hat{y} \right\rangle \right\| \sqrt{4 + L'^2} \end{aligned}$$

Comparing this to (3), we see that we will be done if we show $\left\| \left\langle \frac{\hat{L}}{2}, -\hat{y} \right\rangle \right\| = r$. This vector depends only on the properties of the circle, and again examining Figure 2, we see that $\left\langle \frac{\hat{L}}{2}, -\hat{y} \right\rangle$ is in fact a radius of the circle. q.e.d.

This proof generalizes to spheres. In $\mathbb{R}^n$ the metacalibrating function is $\frac{1}{r}(nV - \hat{x}_n A)$, where $A(t)$ is the $(n-1)$-dimensional area of cross sections cut by hyperplanes planes $x_n = t$, and $V(t)$ is the amount of enclosed volume beneath these planes [**3**].

2. The Tetrahedral Soap Complex

The shapes made by soap films on different wire frames provide a wide variety of interesting candidates for minimization proofs. A regular tetrahedral wire frame, when dipped in a soap solution, forms a film consisting of six planar triangles which come from the edges of the frame and meet at a singular point in the center. Jean Taylor showed in 1976 that this configuration is in fact surface area minimizing [**7**]. Frank Morgan and the second author provided another proof in [**4**] using paired calibrations. The proof can be described essentially as follows: Take four constant vector fields of the same magnitude, each perpendicular to a face of a fixed tetrahedron T, pointing inward. Think of the vectors as rays from four heat lamps. Place the tetrahedral cone into this configuration (with boundary where the edges of T were) and let the lamps heat up its six triangles. Then take out the cone and replace it with any competitor, letting the lamps heat up the competitor's surfaces for the same amount of time as they did the cone.

Now because the boundaries coincided, both the cone and its competitor absorbed equal amounts of energy. On the other hand, each of the cone triangles is tilted in just the ideal direction for it to absorb as much heat as possible from the two lamps it faces. In summary: equal total energy but point wise hotter means that the cone must have less mass over which to distribute the heat.

Now suppose we add a small bubble to the center of the tetrahedral soap film. We now have a variation on the configuration described above. The new shape has an additional constraint — it must enclose a certain volume. The standard bubble in a tetrahedron is shown in Figure 1. It has a subset of the same six planar triangles, but the volume in the center is enclosed by four spherical sections. The center of curvature of each of these spheres is the singular point where the three other spherical sections meet. In standard soap bubbles and films like this, surfaces meet at 120°, and curves meet at about 109.5°.

Taylor's proof for the tetrahedral soap film used process of elimination and is very specific to cones. This type of method may be difficult to apply to more general surfaces, like the bubble in the tetrahedron described here. Applying a traditional calibration also seems to be troublesome. The proof that we present here uses our generalization of calibrations.

This figure is somewhat of a hybrid between a soap film and a soap bubble, so we will call it a soap complex. The following notation will be convenient:

NOTATION. For $0 \leq r \leq s$, $s \neq 0$, let $\mathcal{T}_{r,s}$ designate the standard tetrahedral soap complex described above, with side length of the tetrahedron s and radii of curvature of the spherical sections equal to r. We will orient the tetrahedron so that one vertex is at the origin, and the positive z-axis passes orthogonally through the face opposite that vertex.

The following theorem is the main result of the paper. It claims that $\mathcal{T}_{r,s}$ is the minimal surface area way to "connect" the edges of the tetrahedron and enclose the volume.

Theorem 2.1. *Consider the regular tetrahedron with side length s, oriented as described above. Let $\mathcal{V}$ be the amount of volume enclosed by $\mathcal{T}_{r,s}$, for $r \leq s$. Then, among all integral currents whose support encloses volume $\mathcal{V}$ and intersects every circle linked with the 1-skeleton of the tetrahedron, $\mathcal{T}_{r,s}$ has the minimal surface area.*

The proof for the circle in Theorem 1.2 required us to think about the properties of cross sections of competitors. Since these were fairly simple one dimensional pictures (Figure 3), this was a straightforward task. However, when we consider our three dimensional soap complex, we will be forced to consider properties of cross sections which are two dimensional and relatively complex. The general case is described in the following problem, which is interesting in its own right.

Problem 2.2. Given three vertices of an equilateral triangle and a specified area, find the minimal weighted perimeter way to span the three points and enclose the given area, applying weights as follows.

As shown in Figure 4, let T_1 be the region bounded by the figure and the vertical rays starting from the upper vertices of the equilateral triangle. Let T_2 be the union of regions enclosed by the figure that are not bubble regions, T_3 be the bubble region, T_0 be the union of the remaining regions, and T_{01} be the union of T_1 and T_0. Let B_2 be the union of curves that separate T_2 from T_{01}, B_3 be the union of curves that separate T_2 from T_3, B_4 be the union of curves that separate T_3 from T_{01}, and B_1 be the union of the remaining curves. Also let P_i be the (unweighted) length of the curves in B_i.

Apply the weight w_i when measuring curve B_i, so the weighted perimeter is

$$\mathcal{W} = \sum_{i=1}^{4} w_i P_i.$$

Proposition 2.3 gives a lower bound for a special case of this problem when the weights and area are related to a cross section of $\mathcal{T}_{r,s}$. In this case we will obatin the minimizer from the cross section. Some representative cross sections of $\mathcal{T}_{r,s}$ are shown in Figure 5, when it is sliced by the plane $z = \hat{z} + \frac{\sqrt{6}}{4}s + \frac{\sqrt{3}}{6}r$. This result will provide a lower bound for the derivative of surface area in the proof of the main theorem.

Proposition 2.3. *Let $0 \leq r \leq s$, $s \neq 0$, be given. Let $\hat{z}$ be given so that the slicing plane $z = \hat{z} + \frac{\sqrt{6}}{4}s + \frac{\sqrt{3}}{6}r$ intersects the bubble in $\mathcal{T}_{r,s}$. Let $\lambda \geq 0$ be given. Let $\mathcal{A}$ be the amount of two dimensional area of the intersection of the bubble in $\mathcal{T}_{r,s}$ with the slicing plane above.*

Then, for the situation described in Problem 2.2, with area constraint equal to $\mathcal{A}$, distance from the center of the given equilateral triangle to a vertex equal

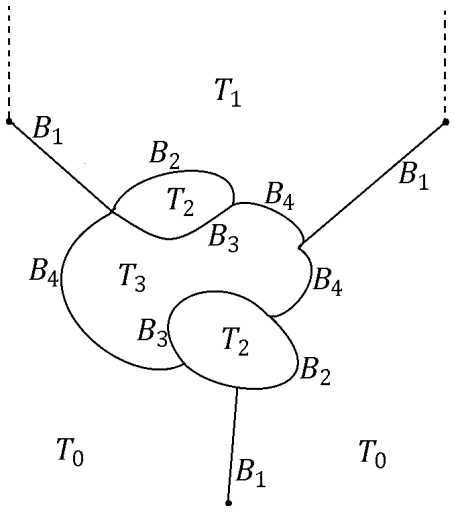

Figure 4. Labeling regions (T_i) and curves (B_i) in Problem 2.2.

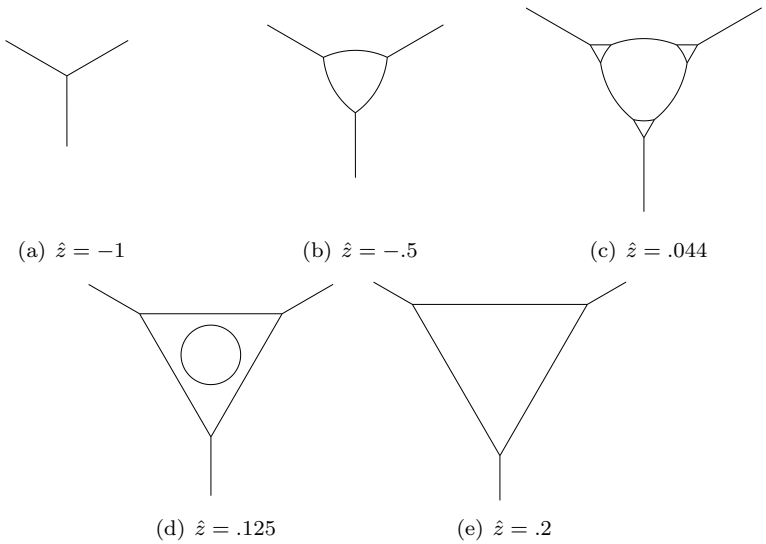

Figure 5. Some cross sections of $\mathcal{T}_{1,3}$ for representative values of $\hat{z}$.

to λ*, and weights* $w_1, \ldots, w_4$ *given by*

$$1, \ \sqrt{\frac{1}{3}}, \ \frac{1}{r}\sqrt{r^2 - \left(\hat{z} + r\sqrt{\frac{2}{3}}\right)^2}, \ \frac{1}{r}\sqrt{r^2 - \hat{z}^2},$$

respectively, the weighted perimeter is at least $3\lambda + 2\frac{A}{r}$.

If the area constraint is zero (so that only the first two weights are relevant), then the weighted perimeter is at least 3λ.

Before we continue, we give a few words of explanation and commentary. In $\mathcal{T}_{r,s}$, the three upper centers of curvature are in the plane $z = \frac{\sqrt{6}}{4}s + \frac{\sqrt{3}}{6}r$. Thus, $\hat{z}$ is the signed distance from the slicing plane to the plane containing the three upper centers of curvature in $\mathcal{T}_{r,s}$. This will be convenient later.

The hypothesis on $\hat{z}$ will ensure that the weights are real.

The case $\lambda = 0$ corresponds to having no boundary constraint.

The case when the area constraint is zero corresponds to slices that do not intersect the bubble. In these cases, the minimal weighted perimeter is 3λ, which is the length of a standard three-point Steiner tree. That is, despite the addition of a weight for a different classification of curve, the Steiner tree is still a minimizer. However, the weights do allow some alternate configurations which have the same weighted perimeter as the Steiner tree, such as the triangle in the center, as seen in Figure 5(e).

The configuration with the triangle surrounding the bubble (Figure 5(d)) is somewhat intriguing. On first inspection, it may seem that eliminating the triangle and connecting directly to the bubble would be more efficient, but doing so changes the classification of the perimeter of the bubble to a more expensive weight.

In order to use emulation, we would like to use a slice of $\mathcal{T}_{r,s}$ as the conjectured minimizer. However, λ, the radius of the triangle to be spanned, is chosen independently of $\mathcal{T}_{r,s}$ and the slicing height $\hat{z}$, thus, it may not exactly match the size of the triangle in the slice at $\hat{z}$. We may need to modify the slice slightly to find a figure μ that has the perimeter of the conjectured lower bound. If the cross section of $\mathcal{T}_{r,s}$ at $\hat{z}$ can have its "arms" cropped or extended to satisfy the constraints, we will let μ be the cropped or extended figure. In this case, it is indeed true that the weighted perimeter of μ is exactly $3\lambda + 2\frac{\mathcal{A}}{r}$. If λ is too small, then we let μ be the cross sectional figure with the arms completely cropped off, centered on the triangle. In this case, it will satisfy only the area constraint and not the spanning constraint, and will actually have weighted perimeter greater than $3\lambda + 2\frac{\mathcal{A}}{r}$, but if we show that it has less weighted perimeter than any figure which satisfies both constraints, we still have found a lower bound. This is only a slight modification of the metacalibration proposition (1.1). Our claims here about the weighted perimeter of μ are verified in the last section as Proposition 3.1.

Proof of Proposition 2.3. The second claim is almost a special case of the first, and the proof is obtained from what follows by ignoring the terms involving the bubble.

Let $\bar{S}$ be the set of all figures that satisfy the constraints. Take the dense subset S, as in Theorem 1.2, to be the the set of piecewise linear figures which satisfy the constraints and have no horizontal line segments. Given any $\sigma \in \bar{S}$, define $\mathcal{W}(\sigma)$ be the weighted perimeter of σ. For $\sigma \in S$, let $W_\sigma(t)$ be the amount of weighted perimeter below a slicing line $y = t$. (These of course take the place of $\mathcal{P}$ and P_σ, respectively.) These functions clearly satisfy condition (1) of Proposition 1.1, if we choose $t^0_\sigma = \inf\{t : y = t \text{ intersects } \sigma\}$ and $t^1_\sigma = \sup\{t : y = t \text{ intersects } \sigma\}$.

Given a competitor sliced by the line $y = t$, let $L_1(t)$, $L_2(t)$, and $L_3(t)$ be the lengths of the intersection of the slicing line with T_1, T_2, and T_3, respectively, and $A(t)$ be the amount of area of the bubble, T_3, beneath the slicing line.

Orient the figure so one vertex of the equilateral triangle is at the origin, and the altitude lies along the positive y-axis. Then, the set of values of t for which the line $y = t$ intersects the triangle is $\left[0, \frac{3}{2}\lambda\right]$.

Now, we use emulation. Recall, as discussed above, that μ was a figure with weighted perimeter greater than or equal to the lower bound. For any t so that the slicing line is not completely above or below the competitor, slice μ with a line so that the amount of bubble area beneath the slicing line is $A(t)$, thus equaling the amount of bubble area beneath the slicing line in the competitor. Let $\hat{y}(t)$ be the signed height of this line. However, we wish to use a different origin for convenience in later calculations. Translate the old origin (described in the previous paragraph) upward by $\lambda + \frac{r}{2}$. Now the line $y = 0$ is the line where centers of curvature of certain curves in μ lie. Let $\hat{L}_3(t)$ be the length of the intersection of the slicing line in μ with T_3, the bubble region.

Define the truncation function:

$$h(t) = \begin{cases} \frac{3}{2}\lambda & t > \frac{3}{2}\lambda \\ t & 0 \le t \le \frac{3}{2}\lambda \\ 0 & t < 0 \end{cases},$$

noting that $h'(t) = \chi_{[0,\frac{3}{2}\lambda]}$, where χ_I is the indicator function of a set I; that is $\chi_I(t) = 1$ if $t \in I$ and $\chi_I(t) = 0$ if $t \notin I$.

We are now ready ready to apply metacalibration.

We claim that the function

$$g(t) = h(t) + \frac{\sqrt{3}}{2}L_1 + \frac{\sqrt{3}}{6}L_2 + \frac{1}{r}\left(2A - \hat{y}L_3\right) \tag{4}$$

satisfies the conditions of Proposition 1.1, and thus metacalibrates μ. Here again we have suppressed the dependence of L_1, L_2, L_3, A, and $\hat{y}$ on t and σ. Notice that although $\hat{y}$ is not defined for all t, it is defined for all t so that $L_3(t) \neq 0$.

To verify the conditions of Proposition 1.1, note that g is indeed continuous and has a derivative that exists except at finitely many points and is bounded, as it is the sum of functions with these properties.

Recall that t_0 is chosen so that $y = t_0$ is below the figure. Thus, each L_i and A are zero at t_0, so $g(t_0) = 0$. Also t_1 is chosen so that $y = t_1$ is above the figure, thus, at t_1, $L_2 = L_3 = 0$, $A = \mathcal{A}$, and $L_1 = \sqrt{3}\lambda$, so $g(t_1) = 3\lambda + 2\frac{\mathcal{A}}{r}$. We have satisfied condition (1).

The next order of business to to calculate g'. Differentiating (4) yields

$$\begin{aligned} g'(t) &= \chi_{[0,\frac{3}{2}\lambda]} + \frac{\sqrt{3}}{2}L_1' + \frac{\sqrt{3}}{6}L_2' + \frac{1}{r}\left(2L_3 - \hat{y}'L_3 - \hat{y}L_3'\right) \\ &= \chi_{[0,\frac{3}{2}\lambda]} + \frac{\sqrt{3}}{2}L_1' + \frac{\sqrt{3}}{6}L_2' + \frac{1}{r}\left(\left(2 - \hat{y}'\right)L_3 - \hat{y}L_3'\right). \end{aligned}$$

This formula is valid except at finitely many points where g' does not exist.

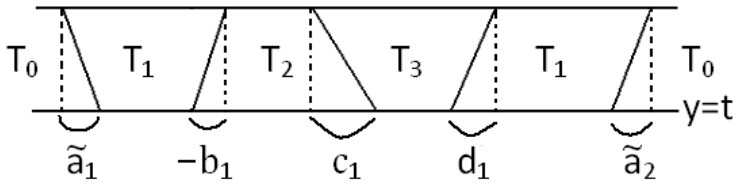

Figure 6. Measuring the horizontal change of curves in a slice.

Now, note that $L_3 = A'(t) = \hat{y}'(t) \cdot \frac{d}{d\hat{y}} A(t) = \hat{y}' \hat{L}_3$. Substitution yields

$$g'(t) = \chi_{[0,\frac{3}{2}\lambda]} + \frac{\sqrt{3}}{2} L_1' + \frac{\sqrt{3}}{6} L_2' + \frac{1}{r} \left((2 - \hat{y}')\, \hat{y}' \hat{L}_3 - \hat{y} L_3' \right) \tag{5}$$

Maximizing with respect to $\hat{y}'$, we get

$$g'(t) \leq \chi_{[0,\frac{3}{2}\lambda]} + \frac{\sqrt{3}}{2} L_1' + \frac{\sqrt{3}}{6} L_2' + \frac{1}{r} \left(\hat{L}_3 - \hat{y} L_3' \right) \tag{6}$$

Now need a way to get a lower bound on $W'(t)$. Consider a competitor sliced at $y = t$. We can slice it with a nearby line, $y = t + \Delta t$. Make Δt small enough that we have linearity (recall that the competitor we are slicing is piecewise linear), then for convenience rescale so $\Delta t = 1$. We will need some creative labeling to measure the horizontal change Δx of each piece of curve between $y = t$ and $y = t + \Delta t$ and to classify them based on the types of regions each piece of curve divides. Let

- $\tilde{a}_1, \ldots, \tilde{a}_{n_{\tilde{a}}}$ be Δx for B_1 that divides T_0 from T_1.
- $b_1, \ldots, b_{n_b}$ be Δx for B_2 that divides T_1 from T_2.
- $\tilde{b}_1, \ldots, \tilde{b}_{n_{\tilde{b}}}$ be Δx for B_2 that divides T_0 from T_2.
- $c_1, \ldots, c_{n_c}$ be Δx for B_3 (that divides T_2 from T_3).
- $d_1, \ldots, d_{n_d}$ be Δx for B_4 that divides T_1 from T_3.
- $\tilde{d}_1, \ldots, \tilde{d}_{n_{\tilde{d}}}$ be Δx for B_4 that divides T_0 from T_3.
- $e_1, \ldots, e_{n_e}$ be Δx for B_1 that divides T_0 from T_0.

where $n_{\tilde{a}}$, n_b, etc. are the number of times the slice intersects the curves of the associated type. (Each of these is finite, since we are slicing piecewise linear figures with no horizontal line segments.) Note that any curve which divides one of the regions T_1, T_2 or T_3 from itself is extraneous and may be removed while still satisfying the constraints. Let these distances Δx be signed by the arbitrary convention that for each line, the direction towards the region with higher index is positive (in the case of e_i the sign is irrelevant). Figure 6 gives an example illustrating this nomenclature. Any of the indexed sets in the above lists may be empty. In that case, simply ignore their respective parts in the following calculations. We can now easily see that the change in weighted

perimeter as the slicing line moves from t to $t+\Delta t$ is

$$\begin{aligned}\Delta W = &\sum\sqrt{1+a_i^2}+\sum\sqrt{1+\tilde{a}_i^2}\\ &+\sqrt{\frac{1}{3}}\left(\sum\sqrt{1+b_i^2}+\sum\sqrt{1+\tilde{b}_i^2}\right)\\ &+\frac{1}{r}\sqrt{r^2-\left(\hat{z}+r\sqrt{\frac{2}{3}}\right)^2}\sum\sqrt{1+c_i^2}\\ &+\frac{1}{r}\sqrt{r^2-\hat{z}^2}\left(\sum\sqrt{1+d_i^2}+\sum\sqrt{1+\tilde{d}_i^2}\right)+\sum\sqrt{1+e_i^2}\end{aligned}\tag{7}$$

Also, with our signing convention, we can conveniently say:

$$\begin{aligned}\Delta L_1 &= -\sum\tilde{a}_i+\sum b_i+\sum d_i\\ \Delta L_2 &= -\sum\tilde{b}_i-\sum b_i+\sum c_i\\ \Delta L_3 &= -\sum c_i-\sum\tilde{d}_i-\sum d_i\end{aligned}$$

Since the curves are linear, if Δt is chosen small enough, then these expressions are also $W'(t)$, L_1', L_2', and L_3'.

Now, from (6), we can write another upper bound for g' as a sum of dot products, assuming for now that it is not the case that both L_3 is identically zero from t to $t+\Delta t$ and $\hat{L}_3\neq 0$:

$$g'(t)\leq\chi_{[0,\frac{3}{2}\lambda]}+\frac{\sqrt{3}}{2}L_1'+\frac{\sqrt{3}}{6}L_2'+\frac{1}{r}\left(\hat{L}_3-\hat{y}L_3'\right)\tag{8}$$

$$\leq\left\langle\frac{1}{2},\frac{\sqrt{3}}{2}\right\rangle\cdot\sum\langle 1,-\tilde{a}_i\rangle\tag{9}$$

$$+\left\langle 0,\frac{\sqrt{3}}{2}-\frac{\sqrt{3}}{6}\right\rangle\cdot\sum\langle 1,b_i\rangle\tag{10}$$

$$+\left\langle\frac{1}{2},-\frac{\sqrt{3}}{6}\right\rangle\cdot\sum\left\langle 1,\tilde{b}_i\right\rangle\tag{11}$$

$$+\frac{1}{r}\left\langle\frac{\hat{L}_3}{n_c+n_d+n_{\tilde{d}}},\hat{y}+\frac{r\sqrt{3}}{6}\right\rangle\cdot\sum\langle 1,c_i\rangle\tag{12}$$

$$+\frac{1}{r}\left\langle\frac{\hat{L}_3}{n_c+n_d+n_{\tilde{d}}},\hat{y}+\frac{r\sqrt{3}}{2}\right\rangle\cdot\sum\langle 1,d_i\rangle\tag{13}$$

$$+\frac{1}{r}\left\langle\frac{\hat{L}_3}{n_c+n_d+n_{\tilde{d}}}+\frac{r}{2},\hat{y}\right\rangle\cdot\sum\left\langle 1,\tilde{d}_i\right\rangle+n_e\tag{14}$$

If $n_c=n_d=n_{\tilde{d}}=0$, that is, $L_3=0$ on $[t,t+\Delta t]$, then omit the last three dot products.

To see that the inequality in (9) is true, we consider several cases. First, consider the case where it is not true that each L_i is zero on $[t, t+\Delta t]$. That is, the slicing line intersects some region other than T_0. Then $n_{\tilde{a}} + n_{\tilde{b}} + n_{\tilde{d}}$ is at least 2, as the tildes indicate curves that border T_0, and T_0 has at least two non-adjacent components in this type of slice. Therefore, the contribution of constants from (9), (11), and (14) is at least 1, which balances out $\chi_{[0,\frac{3}{2}\lambda]}$. As long as L_3 is not zero on $[t, t+\Delta t]$, the contribution of $\hat{L}_3$ by (12), (13), and (14) is $\frac{1}{r}\hat{L}_3$. Next, (9), (10), and (13) contribute $\frac{\sqrt{3}}{2}\left(-\sum \tilde{a}_i + \sum b_i + \sum d_i\right) = \frac{\sqrt{3}}{2}L_1'$, while (10), (11), and (12) contribute $\frac{\sqrt{3}}{6}\left(-\sum b_i - \sum \tilde{b}_i + \sum c_i\right) = \frac{\sqrt{3}}{6}L_2'$. Finally, from (12), (13), and (14), we get $-\hat{y}\frac{1}{r}\left(-\sum c_i - \sum \tilde{d}_i - \sum d_i\right) = -\frac{1}{r}\hat{y}L_3'$. There is nothing left over, except possibly a positive contribution to the right hand side by n_e, so the inequality is satisfied. In cases where some of the L_i are identically 0 on $[t, t+\Delta t]$, we find that exactly the right things drop out of each side.

In the case where each L_i is identically zero on $[t, t+\Delta t]$, we will have $L_i' = 0$. Then, if $t \in \left[0, \frac{3}{2}\lambda\right]$, that is, the slice intersects the triangle, then (8) boils down to $1 \leq n_e$, which is true because any such slice that does not intersect any of T_1, T_2, or T_3 must intersect B_1 at least once, or the figure could not span the triangle. If the slice doesn't go through the triangle, we have $0 \leq n_e$.

Now, consider the case where L_3 is identically zero from t to $t+\Delta t$ and $\hat{L}_3$ is not 0. Geometrically, this means that the bubble in the competitor is disconnected, and the current slicing line lies between separate pieces of it. Then, lines (12) through (14) drop out, but we still have $\hat{L}_3$ on the left side of the inequality. In this case, we have thrown too much away when we maximized with respect to $\hat{y}'$ in (6). So instead, note that if $L_3 = 0$ on $[t, t+\Delta t]$, then $0 = A' = \hat{y}'\hat{L}_3$ and $L_3' = 0$. Equation (5) then gives us

$$g'(t) = \chi_{[0,\frac{3}{2}\lambda]} + \frac{\sqrt{3}}{2}L_1' + \frac{\sqrt{3}}{6}L_2'$$

and thus g' still satisfies the inequality.

Now we would like to apply the Cauchy-Schwartz inequality as we did in the circle proof. Consider the first vector in the dot product on line (12). We claim

$$\left\| \left\langle \frac{\hat{L}_3}{n_c + n_d + n_{\tilde{d}}}, \hat{y} + \frac{r\sqrt{3}}{6} \right\rangle \right\| \leq \left\| \left\langle \frac{\hat{L}_3}{2}, \hat{y} + \frac{r\sqrt{3}}{6} \right\rangle \right\| \tag{15}$$

This is because $n_c + n_d + n_{\tilde{d}}$ represents the number of times a boundary of the bubble is intersected by the slicing line. If it is crossed at all, it must be crossed at least twice.

The vector on the right hand side of (15) depends only on properties of the ideal figure μ. Now, μ may have two kinds of circular arcs — the first have centers of curvature that form an equilateral triangle with side length r. These are labeled D_1 through D_3 in Figures 7 through 9. Two of these lie in the line $y = 0$, the line from which $\hat{y}$ is measured from, and the third is below them. The arcs associated with these centers of curvature have radii of curvature $\sqrt{r^2 - \hat{z}^2}$. Another center of curvature is the center of μ (labeled C)

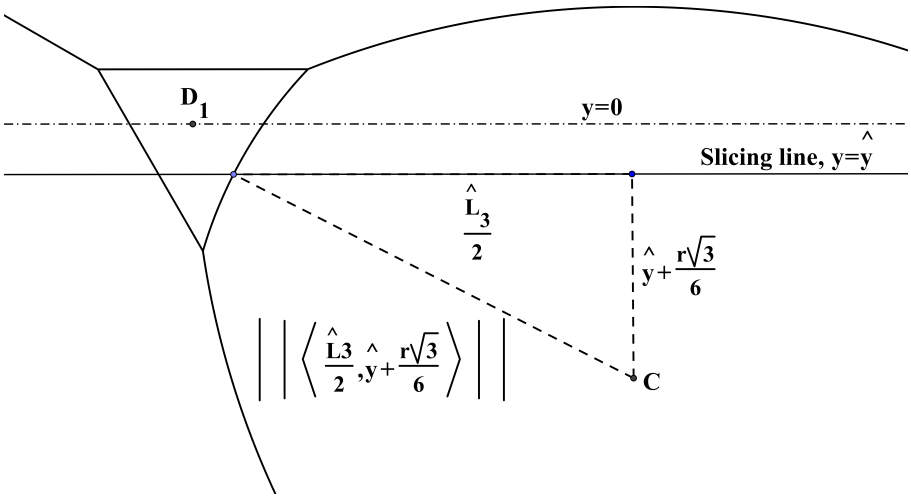

Figure 7. $\left\|\left\langle \frac{\hat{L}_3}{2}, \hat{y} + \frac{r\sqrt{3}}{6} \right\rangle\right\| \leq \sqrt{r^2 - \left(\hat{z} + r\sqrt{\frac{2}{3}}\right)^2}$

and the associated arcs have radius $\sqrt{r^2 - \left(\hat{z} + r\sqrt{\frac{2}{3}}\right)^2}$. These facts can be verified by thinking of μ as a cross section of $\mathcal{T}_{r,s}$. Examining Figure 7, recall that the distance from the center C of the equilateral triangle with side length r to an edge of the triangle is $\frac{r\sqrt{3}}{6}$, and thus the distance from the center C to the slicing line is $\frac{\sqrt{3}}{6} + \hat{y}$. The distance from the center of the slicing line to the edge of the bubble is $\frac{\hat{L}_3}{2}$ by the definition of $\hat{L}_3$. These two segments form a right triangle with hypotenuse of length $\left\|\left\langle \frac{\hat{L}_3}{2}, \hat{y} + \frac{r\sqrt{3}}{6} \right\rangle\right\|$. This hypotenuse is also a radius of the smaller circle arcs which have center of curvature at C. Thus, we see that in this case, $\sqrt{r^2 - \left(\hat{z} + \sqrt{\frac{2}{3}}\right)^2} = \left\|\left\langle \frac{\hat{L}_3}{2}, \hat{y} + \frac{r\sqrt{3}}{6} \right\rangle\right\|$. The explanations for Figures 8 and 9 are similar. The only additional subtlety is demonstrated in Figure 8, though it may occur in any of these cases. The vector on the right hand side of (15) may not actually be a radius— but if that is the case, it is always shorter that a vector that is a radius.

Now that we have bounds on the norms of the vectors on the right hand side of (8), we are ready to apply the Cauchy-Schwartz inequality, and noting that certainly $1 \leq \sqrt{1 + e_i^2}$, we see that

$$\begin{aligned} g'(t) \leq & \sum \sqrt{1 + a_i^2} + \sum \sqrt{1 + \tilde{a}_i^2} + \sqrt{\frac{1}{3}} \left(\sum \sqrt{1 + b_i^2} + \sum \sqrt{1 + \tilde{b}_i^2} \right) \\ & + \frac{1}{r} \sqrt{r^2 - \left(\hat{z} + r\sqrt{\frac{2}{3}} \right)^2} \sum \sqrt{1 + c_i^2} \\ & + \frac{1}{r} \sqrt{r^2 - \hat{z}^2} \left(\sum \sqrt{1 + d_i^2} + \sum \sqrt{1 + \tilde{d}_i^2} \right) + \sum \sqrt{1 + e_i^2} \end{aligned}$$

which is exactly $W'(t)$ from (7). q.e.d.

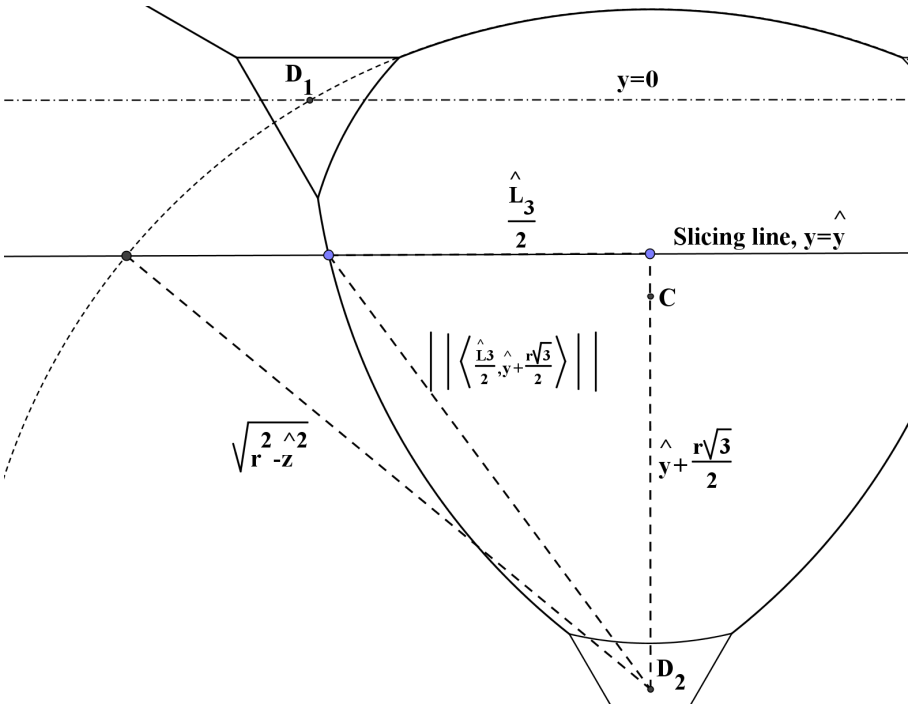

Figure 8. $\left\|\left\langle \frac{\hat{L}_3}{2}, \hat{y} + \frac{r\sqrt{3}}{2} \right\rangle\right\| \leq \sqrt{r^2 - \hat{z}^2}$

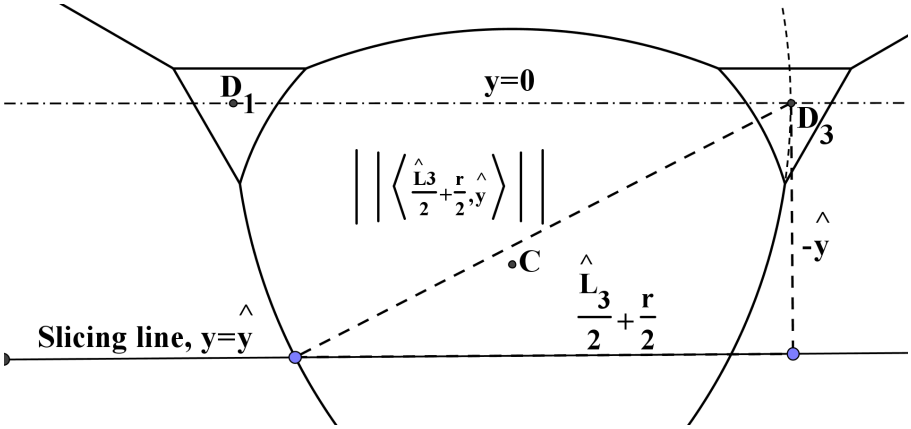

Figure 9. $\left\|\left\langle \frac{\hat{L}_3}{2} + \frac{r}{2}, \hat{y} \right\rangle\right\| \leq \sqrt{r^2 - \hat{z}^2}$

Armed with Proposition 2.3, we are ready to proceed to the main theorem.

Proof of Theorem 2.1. As before, we take our dense subset S of the competitors to be those that are piecewise linear surfaces with no horizontal planar pieces.

For any competitor, let $\Sigma(t)$ be the amount of surface area lying below the slicing plane $z = t$. Let $V(t)$ be the amount of the bubble's volume lying below the slicing plane. Let $A_B(t)$ be the cross sectional area of the bubble with the slicing plane. Take the top face of the tertrahedron, and extend it infinitely in both directions to a right triangular prism. The portion of this prism that lies above the figure call R_T, and let $A_T(t)$ be the cross sectional area of this top region R_T.

Again, we use emulation and define our hat functions by slicing $\mathcal{T}_{r,s}$ by a plane so that the amount of bubble volume underneath the plane is the same as that in the competitor. Then $\hat{z}(t)$ is defined to be the signed distance from this slicing plane to the plane formed by the three upper centers of curvature, $z = \frac{\sqrt{6}}{4}s + \frac{\sqrt{3}}{6}r$. Finally, $\hat{A}_B(t)$ is the amount of two dimensional area of the intersection of the bubble in $\mathcal{T}_{r,s}$ with the slicing plane.

Again, define a truncation function:

$$h(t) = \begin{cases} \frac{\sqrt{2}}{2}s^2 & t \geq s\sqrt{\frac{2}{3}} \\ \sqrt{\frac{9}{8}}t^2 & t \in \left(0, s\sqrt{\frac{2}{3}}\right) \\ 0 & t \leq 0 \end{cases}$$

Now, we claim the function

$$g(t) = h(t) + \sqrt{\frac{2}{3}}A_T + \frac{1}{r}\left(3V - \hat{z}A_B\right) \tag{16}$$

metacalibrates $\mathcal{T}_{r,s}$.

Notice that $\hat{z}$ is well defined only for t where the slicing plane is not completely above or below the bubble, but when $\hat{z}$ is not well defined, $A_B = 0$, so the product $A_B\hat{z}$ is defined for all t.

Next, note that g is indeed continuous. Then, as usual, we choose t_0 below the figure and t_1 above. Since t_0 is below the figure, $g(t_0) = 0$. Since t_1 is above the figure, $A_T = \frac{\sqrt{3}}{4}s^2$, and we have $g(t_1) = \frac{3\sqrt{2}}{4}s^2 + \frac{3}{r}\mathcal{V}$. Thus we get that $g(t_1) - g(t_0) = \frac{3\sqrt{2}}{4}s^2 + \frac{3}{r}\mathcal{V}$ for any competitor. This is the surface area of $\mathcal{T}_{r,s}$. This fact is verified in Section 3, Proposition 3.3.

Differentiating (16), noting that $V' = A_B$ and grouping terms yields

$$g'(t) = 2\sqrt{\frac{9}{8}}t\chi_{[0,s\sqrt{\frac{2}{3}}]} + \sqrt{\frac{2}{3}}A_T' + \frac{1}{r}\left(3A_B - \hat{z}A_B' - \hat{z}'A_B\right) \tag{17}$$

$$= \frac{3\sqrt{2}}{2}t\chi_{[0,s\sqrt{\frac{2}{3}}]} + \sqrt{\frac{2}{3}}A_T' + \frac{1}{r}\left(\left(3 - \hat{z}'\right)A_B - \hat{z}A_B'\right) \tag{18}$$

Now, note that, using the chain rule, $A_B = V'(z) = \frac{d}{d\hat{z}}V(t) \cdot \hat{z}'(t) = \hat{A}_B\hat{z}'$. But this time we will split A_B into $\sqrt{A_B}\sqrt{A_B}$ before substituting:

$$g'(t) = \frac{3\sqrt{2}}{2}t\chi_{[0,s\sqrt{\frac{2}{3}}]} + \sqrt{\frac{2}{3}}A_T' + \frac{1}{r}\left(\left(3 - \hat{z}'\right)\sqrt{\hat{z}'\hat{A}_BA_B} - \hat{z}A_B'\right)$$

Treating $\hat{z}'$ as an independent variable and maximizing $\left(3 - \hat{z}'\right)\sqrt{\hat{z}}$, we find that

$$g'(t) \leq \frac{3\sqrt{2}}{2}t\chi_{[0,s\sqrt{\frac{2}{3}}]} + \sqrt{\frac{2}{3}}A_T' + \frac{1}{r}\left(2\sqrt{\hat{A}_BA_B} - \hat{z}A_B'\right) \tag{19}$$

We would now like to compare $g'(t)$ to $\Sigma'(t)$. To get a lower bound on $\Sigma'(t)$, we need a slicing lemma.

Lemma 2.4 (Slicing Lemma)**.** *Let D be a piecewise linear surface with no horizontal planar sections that encloses and separates two (possibly disconnected) regions.*

Slice D with the plane $z = t$ and let $A_1(t)$, $A_2(t)$ be the amounts of the two dimensional cross sectional areas of the respective regions. Let $P_1(t)$, $P_2(t)$ be the respective lengths of the one dimensional cross sections of the surface that divide the enclosed regions from the outside, and $P_{12}(t)$ be the length of the one dimensional cross section of the boundary between the two enclosed regions. Let $\Sigma(t)$ be the amount of surface area of the surface lying below the slicing plane.

Then, for all t and any $\alpha_i, \beta_i \geq 0$, $i = 1, 2$ with $\alpha_i^2 + \beta_i^2 = 1$ and $\beta_1 + \beta_2 \leq 1$, we have

$$\Sigma' \geq \alpha_1 |A_1'| + \beta_1 P_1 + \alpha_2 |A_2'| + \beta_2 P_2 + \sqrt{1 - (\beta_1 + \beta_2)^2} P_{12}$$

Proof. First, for a general surface (not necessarily enclosing volumes) being sliced, we define $B(t)$ to be the one dimensional cross section of the surface, with $B[a, b] = \bigcup_{t \in [a,b]} B(t)$. Then we define

$$W(t) = \lim_{h \to 0} \frac{1}{h} \text{Area}\left(\Pi\left(B[t, t + h]\right)\right)$$

where Π is projection onto the plane $z = 0$.

Now we claim, for $\alpha^2 + \beta^2 = 1$,

$$\Sigma'(t) \geq \alpha W(t) + \beta P(t)$$

(where $P(t)$ is the length of $B(t)$).

This is easy to show for linear surfaces, and since the inequality is linear, it is also true for piecewise linear surfaces.

Now, for the surface described in the statement of the lemma, we let W_1, W_2, and W_{12} be the W functions for the corresponding pieces of surface. Note that we have

$$|A_1'| \leq W_1 + W_{12}$$
$$|A_2'| \leq W_2 + W_{12}$$

Now, by adding the three pieces together and applying the previous result, we get

$$\begin{aligned}\Sigma' &\geq \alpha_1 P_1 + \beta_1 W_1 + \alpha_2 P_2 + \beta_2 P_2 + (\beta_1 + \beta_2) W_{12} + \sqrt{1 - (\beta_1 + \beta_2)^2} P_{12} \\ &\geq \alpha_1 |A_1'| + \beta_1 P_1 + \alpha_2 |A_2'| + \beta_2 P_2 + \sqrt{1 - (\beta_1 + \beta_2)^2} P_{12}\end{aligned}$$

as desired. This completes the proof of Lemma 2.4. q.e.d.

We continue with the proof of Theorem 2.1. Now, we may apply the Slicing Lemma to P_2, P_4, P_3, and A_T', A_B', and get a lower bound on Σ':

(20)

$$\Sigma' \geq P_1 + \sqrt{\frac{1}{3}} P_2 + \frac{1}{r} \sqrt{r^2 - \left(r\sqrt{\frac{2}{3}} + \hat{z}\right)^2} P_3 + \frac{1}{r} \sqrt{r^2 - \hat{z}^2} P_4 + \sqrt{\frac{2}{3}} A_T' - \frac{\hat{z}}{r} A_B'$$

The values of α_i and β_i are chosen so that equality holds for the minimizer, which is a necessary condition for the conditions of Proposition 1.1 to hold. We have dropped some absolute values and changed a sign to put the expression in a convenient form, but these changes preserve the inequality.

Now that we have an lower bound for $\Sigma'(z)$, we would like to compare it with $g'(t)$ to verify condition (4) in the metacalibration proposition (1.1). We hope that $g'(t) \leq \Sigma'(t)$, which will be true if, substituting from (19),

$$\frac{3\sqrt{2}}{2} t\chi_{[0,s\sqrt{\frac{2}{3}}]} + \sqrt{\frac{2}{3}} A'_T + \frac{1}{r}\left(2\sqrt{\hat{A}_B A_B} - \hat{z}A'_B\right)$$

$$\leq P_1 + \sqrt{\frac{1}{3}} P_2 + \frac{1}{r}\sqrt{r^2 - \left(r\sqrt{\frac{2}{3}} + \hat{z}\right)^2} P_3 + \frac{1}{r}\sqrt{r^2 - \hat{z}^2} P_4 + \sqrt{\frac{2}{3}} A'_T - \frac{\hat{z}}{r} A'_B$$

which simplifies to

(21)

$$\frac{3\sqrt{2}}{2} t\chi_{[0,s\sqrt{\frac{2}{3}}]} + \frac{2}{r}\sqrt{A_B \hat{A}_B} \leq P_1 + \sqrt{\frac{1}{3}} P_2 + \frac{1}{r}\sqrt{r^2 - \left(r\sqrt{\frac{2}{3}} + \hat{z}\right)^2} P_3 + \frac{1}{r}\sqrt{r^2 - \hat{z}^2} P_4.$$

We need to find a lower bound for the right hand side of (21). If we look at a geometric interpretation of the quantity, we see that it is very similar to the two dimensional weighted perimeter minimization problem from Proposition 2.3. First assume that $t \in [0, s\sqrt{2/3}]$, that is, the slice $z = t$ intersects the tetrahedron. Then, we need to know the minimum weighted perimeter of any figure which encloses area A_B and spans the vertices of the equilateral triangle with distance from vertex to center $t\frac{\sqrt{2}}{2}$. (The equilateral triangle that needs to be spanned in the cross section of the tetrahedron that must be spanned.) If $\hat{A}_B \neq 0$ and $A_B \neq 0$, we will first apply the proposition to $\hat{z}(t)$, r, and s with $\lambda = \frac{\sqrt{2}}{2} t\sqrt{\hat{A}_B / A_B}$. Then, we can conclude that the minimum weighted perimeter that encloses area $\hat{A}_B$ and spans the three points is $\frac{3\sqrt{2}}{2} t\sqrt{\hat{A}_B / A_B} + \frac{2}{r}\hat{A}_B$. If we dilate this result by a factor of $\sqrt{A_B/\hat{A}_B}$, we dilate the area by the square of the dilating factor and the lengths linearly. Thus, we conclude that a figure that spans three points with distance $\frac{\sqrt{2}}{2}t$ from the center and encloses an area A_B has weighted perimeter at least $\frac{3\sqrt{2}}{2}t + \frac{2}{r}\sqrt{A_B \hat{A}_B}$, satisfying (21), as desired.

If $\hat{A}_B = 0$, note that A_B must also be zero, since the only time $\hat{A}_B$ is zero is when the enclosed volume is completely above or completely below the slicing plane. If $A_B = 0$, then let $\lambda = t\frac{\sqrt{2}}{2}$, and apply the second result in Proposition 2.3.

In the case $t \notin [0, s\sqrt{2/3}]$, then the slice does not intersect the tetrahedron, and there is no boundary constraint, so we may similarly apply Proposition 2.3 with $\lambda = 0$.

q.e.d.

3. Appendix

This section gives the calculations of the weighted perimeter of the ideal figure μ, which is based on a cross section of $\mathcal{T}_{r,s}$, as well as for the surface area of $\mathcal{T}_{r,s}$ itself. The way we obtain these calculations may provide some insight into the choice of the calibrating functions.

Proposition 3.1. *The figure μ described on page 8 with weights as given by Proposition 2.3 has weighted perimeter greater than or equal to $3\frac{\sqrt{2}}{2}t+2\frac{A_B}{r}$. If μ satisfies the spanning constraint, then it has weighted perimeter equal to $3\lambda+2\frac{A_B}{r}$.*

Proof. Assume for now that we have the desired equality. Then, recall that μ may not satisfy the spanning constraint if λ is chosen too small. In this case, μ_λ is the same as some $\mu_{\lambda'}$ that does satisfy the spanning constraint with $\lambda<\lambda'$. Thus $\mathcal{W}(\mu_\lambda)=\mathcal{W}(\mu_{\lambda'})=3\lambda'+2\frac{A_B}{r}>3\lambda+2\frac{A_B}{r}$ as desired.

We now address the case where μ does fit the spanning constraint. In Proposition 2.3, we only defined g for piecewise linear figures. However, we now define it in exactly the same way for μ, which may not be piecewise linear. Our strategy is to show that $g'_\mu=W'_\mu$ wherever the derivatives exists, and then that the only point where they do not exist is due to a jump discontinuity in g and W. We will then argue that this jump discontinuity has the same magnitude for both g and W.

First, note that, from (5), noting that $L_3=\hat{L}_3$, we get

$$\begin{aligned} g'(t) &= \chi_{[0,\frac{3}{2}\lambda]}+\frac{\sqrt{3}}{2}L'_1+\frac{\sqrt{3}}{6}L'_2+\frac{1}{r}\left(\left(2-\hat{y}'\right)L_3-\hat{y}L'_3\right). \\ &= 1+\frac{\sqrt{3}}{2}L'_1+\frac{\sqrt{3}}{6}L'_2+\frac{1}{r}\left(L_3-\hat{y}L'_3\right). \end{aligned}$$

We must divide the analysis into several cases, as shown in Figure 10. For convenience, we use the coordinate system we used for measuring $\hat{y}$.

Case 1. Recall that the derivative of arc length of a differentiable function $f(y)$ is given by $\sqrt{1+[f'(y)]^2}$. If we view the curves in μ as graphs of functions of y, we can say for example in this case that the derivative is $\pm\frac{L'_1}{2}$. By symmetry, $P'(t)=2\sqrt{1+\left[\frac{L'_1}{2}\right]^2}=\sqrt{4+L'^2_1}$. Thus we have

$$\begin{aligned} g'(t) &= 1+\frac{\sqrt{3}}{2}L'_1 \\ &= \left\langle\frac{1}{2},\frac{\sqrt{3}}{2}\right\rangle\cdot\langle 2,L'_1\rangle \\ &= \sqrt{4+L'^2_1} \\ &= W'(t) \end{aligned}$$

Notice that since $L'_1=2\sqrt{3}$, the Cauchy-Schwartz inequality gives equality.

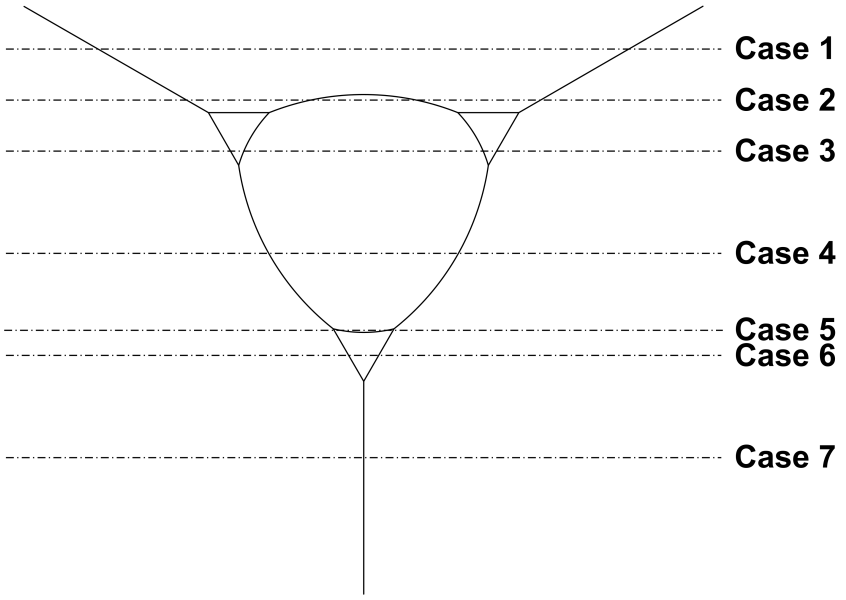

Figure 10. Classifications of slices of cross sections of a tetrahedral soap complex.

Case 2. Notice this time that $L_1' + L_3' = 2\sqrt{3}$. Then, we notice that the vector $\left\langle \frac{L_3}{2}, \hat{y} + \frac{r\sqrt{3}}{2} \right\rangle$ is a radius of one of the larger spherical arcs with radius of curvature $\sqrt{r^2 - \hat{z}^2}$. Also, recall that a normal vector to the graph of a differentiable function $x(y)$ is $\langle 1, -x'(y) \rangle$. Since the derivative of the arc intersected in Case 2, when the arc is viewed as the graph of a function of y, is $\frac{L_3'}{2}$, we see that $\langle 2, -L_3' \rangle$ is normal to the arc on one side. The radius is also normal to the arc on that side; thus Cauchy-Schwartz gives equality.

$$\begin{aligned} g'(t) &= 1 + \frac{\sqrt{3}}{2} L_1' + \frac{1}{r} \left(L_3 - \hat{y} L_3' \right) \\ &= \left\langle \frac{1}{2}, \frac{\sqrt{3}}{2} \right\rangle \cdot \langle 2, L_1' + L_3' \rangle + \frac{1}{r} \left\langle \frac{L_3}{2}, \hat{y} + \frac{r\sqrt{3}}{2} \right\rangle \cdot \langle 2, -L_3' \rangle \\ &= \sqrt{4 + (L_1' + L_3')^2} + \frac{1}{r} \sqrt{r^2 - \hat{z}^2} \sqrt{4 + L_3'} \\ &= W'(t) \end{aligned}$$

Case 3. Notice that $L_2' + L_3' = \frac{2\sqrt{3}}{3}$. Also, $\left\langle \frac{L_3}{2}, \hat{y} + \frac{r\sqrt{3}}{6} \right\rangle$ is a radius of the smaller circular arc, while $\langle 2, -L_3' \rangle$ is normal to that arc.

$$\begin{aligned} g'(t) &= 1 + \frac{\sqrt{3}}{6} L_2' + \frac{1}{r}\left(L_3 - \hat{y} L_3'\right) \\ &= \left\langle \frac{1}{2}, \frac{\sqrt{3}}{6} \right\rangle \cdot \langle 2, L_2' + L_3' \rangle + \frac{1}{r} \left\langle \frac{L_3}{2}, \hat{y} + \frac{r\sqrt{3}}{6} \right\rangle \cdot \langle 2, -L_3' \rangle \\ &= \sqrt{\frac{2}{3}} \sqrt{4 + (L_2' + L_3')^2} + \frac{1}{r} \sqrt{r^2 - \left(\hat{z}^2 + \sqrt{\frac{2}{3}}\right) \sqrt{4 + L_3'}} \\ &= W'(t) \end{aligned}$$

Case 4. Case 4 is a simpler instance of Case 2.

$$\begin{aligned} g'(t) &= 1 + \frac{1}{r}\left(L_3 - \hat{y} L_3'\right) \\ &= \frac{1}{r} \left\langle \frac{L_3}{2} + \frac{r}{2}, \hat{y} \right\rangle \cdot \langle 2, L_3' \rangle \\ &= \frac{1}{r} \sqrt{r^2 - \hat{z}^2} \sqrt{4 + L_3'} \\ &= W'(t) \end{aligned}$$

Case 5. Case 5 is the same as Case 3.

Case 6. Case 6 is a simpler instance of Case 3.

Case 7. Case 7 is trivial.

$$\begin{aligned} g'(t) &= 1 \\ &= W'(t) \end{aligned}$$

Now, notice there is a jump discontinuity in both $W(t)$ and $g(t)$ where there are two horizontal line segments (between Case 2 and Case 3 in Figure 10). Let us call this point $\tilde{t}$. In $g(t)$, this jump is is due to the fact that L_2 jumps to zero and L_1 jumps from zero to the previous value of L_2. Thus the magnitude of this jump is

$$\frac{\sqrt{3}}{2} L_2(\tilde{t}) - \frac{\sqrt{3}}{6} L_2(\tilde{t}) = \sqrt{\frac{1}{3}} L_2(\tilde{t}).$$

In $W(t)$, the jump is caused by the horizontal line segment which has length $L_2(\tilde{t})$ and weight classification $\sqrt{\frac{1}{3}}$. Thus, the jumps are equal as claimed.

Now, we have seen that g and W are continuous except at one point where they have a jump discontinuity of equal magnitude and that g and W are differentiable with bounded derivatives and have the same derivative. Also, we have that $W(t_0) = 0$ and $g(t_0) = 0$. Thus, by the Fundamental Theorem of Calculus, we may conclude that $W(t_1) = g(t_1) = 3\lambda + 2\frac{\mathcal{A}}{r}$. q.e.d.

To address the 3-dimensional case, we need the following Lemma.

Lemma 3.2. *Consider a section of the sphere $x^2 + y^2 + z^2 = R^2$ bounded by two curves defined by*

$$C_i(t) = \left\langle \sqrt{R^2 - t^2}\cos\theta_i(t), \sqrt{R^2 - t^2}\sin\theta_i(t), t \right\rangle$$

for differentiable functions θ_i, $i = 1, 2$. Then, with Σ and P defined as in Lemma 2.4, we have

$$\Sigma'(t) = \frac{1}{R}\sqrt{R^2 - t^2}P(t) + \left|\frac{t}{R}A'(t)\right|$$

Proof. Consider a vector field with unit norm defined by

$$\mathbf{v}(x, y, z) = \frac{1}{R}\left\langle \frac{x\sqrt{R^2 - z^2}}{\sqrt{x^2 + y^2}}, \frac{y\sqrt{R^2 - z^2}}{\sqrt{x^2 + y^2}}, z \right\rangle.$$

Now, consider a strip of the sphere between the planes $z = t$ and $z = t + \Delta t$. Since the vector field $\mathbf{v}$ has unit norm and is normal to the sphere, we know that the surface area of this strip is equal to the flux of $\mathbf{v}$ through it. If we define ΔA to be the amount of two dimensional area of the projection of the strip onto the xy plane, then the flux due to the z component of the vector field is $|t + E_1|\Delta A$, where $|E_1| < \Delta t$. Now, the amount of flux due to the x and y components of the vector field is $\frac{1}{R}\sqrt{R^2 - t^2}(P + E_2)\Delta t$, where

$$\begin{aligned} |E_2| &\leq |r\theta - (r + \Delta r)(\Delta\theta_1 + \Delta\theta_2 + \theta)| \\ &= |r(\Delta\theta_1 + \Delta\theta_2) + \Delta r(\Delta\theta_1 + \Delta\theta_2)| \end{aligned}$$

where $\theta = |\theta_1(t) - \theta_2(t)|$, $r = \sqrt{R^2 - t^2}$, $\Delta r = \sqrt{R^2 - (t + \Delta t)^2} - \sqrt{R^2 - t^2}$, and $\Delta\theta_i = \theta_i(t + \Delta t) - \theta_i(t)$. E_2 is the greatest amount that P could change between t and $t + \Delta t$. Thus, the total flux through the strip of the surface (which is also the surface area of the strip) is

$$\Delta\Sigma = \frac{1}{R}\left(|t + E_1|\Delta A + \sqrt{R^2 - z^2}(P + E_2)\Delta z\right).$$

But note that

$$\begin{aligned} \lim_{\Delta t\to 0}|E_2| &\leq \lim_{\Delta z\to 0} r(\theta_1' + \theta_2')\Delta t + r'(\theta_1' + \theta_2')\Delta t^2 \\ &= 0. \end{aligned}$$

Thus,

$$\begin{aligned} \Sigma' &= \lim_{\Delta t\to 0}\frac{\Delta\Sigma}{\Delta t} \\ &= \lim_{\Delta t\to 0}\frac{1}{\Delta t R}\left(|t + E_1|\Delta A + \sqrt{R^2 - t^2}(P + E_2)\Delta t\right) \\ &= \frac{1}{R}\sqrt{R^2 - t^2}P + \left|\frac{t}{R}A'\right| \end{aligned}$$

as desired. q.e.d.

Proposition 3.3. *If r and s are chosen so that $\mathcal{T}_{r,s}$ is well defined, and $\mathcal{V}$ is the volume of the bubble in $\mathcal{T}_{r,s}$, then the surface area of $\mathcal{T}_{r,s}$ is exactly $\frac{3\sqrt{2}}{4}s^2 + \frac{3}{r}\mathcal{V}$.*

Proof. Recall from (18) that

$$g'(t) = \frac{3\sqrt{2}}{2} t \chi_{[0, s\sqrt{\frac{2}{3}}]} + \sqrt{\frac{2}{3}} A'_T + \frac{1}{r}\left((3 - \hat{z}') A_B - \hat{z} A'_B \right)$$

and in our current case, this reduces to

$$g'(t) = \frac{3\sqrt{2}}{2} t + \sqrt{\frac{2}{3}} A'_T + \frac{1}{r}\left(2A_B - \hat{z} A'_B \right).$$

Now, we claim that equality holds for (20). That is,

(22)

$$\Sigma' = P_1 + \sqrt{\frac{1}{3}} P_2 + \frac{1}{r}\sqrt{r^2 - \left(r\sqrt{\frac{2}{3}} + \hat{z} \right)^2} P_3 + \frac{1}{r}\sqrt{r^2 - \hat{z}^2} P_4 + \sqrt{\frac{2}{3}} A'_T - \frac{\hat{z}}{r} A'_B$$

To see this, consider the four classifications of surface in $\mathcal{T}_{r,s}$. The first are the vertical planes. Their contribution to Σ' is covered by P_1. The next are the spherical sections with centers of curvature in the plane where $\hat{z} = 0$. Their contribution to Σ' is, by Lemma 3.2, $\frac{1}{r}\sqrt{r^2 - \hat{z}^2} P_4 - \frac{\hat{z}}{r} A'_B$. Notice that since A'_B is negative when $\hat{z}$ is positive and vise versa, the effect of the negative sign is to take the absolute value. Then, the top spherical section has center of curvature at $\hat{z} = r\sqrt{\frac{2}{3}}$, so its contribution is $\frac{1}{r}\sqrt{r^2 - \left(r\sqrt{\frac{2}{3}} + \hat{z} \right)^2} P_3 - \frac{1}{r}\left(r\sqrt{\frac{2}{3}} + \hat{z} \right) A'_B$. Notice that A'_B is negative for this part of the surface. At last, easy geometric calculations show that for the upper planar sections of $\mathcal{T}_{r,s}$, the derivative of surface area is $\sqrt{\frac{1}{3}} + \sqrt{\frac{2}{3}}\left(A'_T + A'_B \right)$. Summing these all together gives the desired equality in (22). Now, by Proposition 3.1, since for actual cross sections of $\mathcal{T}_{r,s}$ we know that $\lambda = \frac{\sqrt{2}}{2} t$, we have

$$P_1 + \sqrt{\frac{1}{3}} P_2 + \frac{1}{r}\sqrt{r^2 - \left(r\sqrt{\frac{2}{3}} + \hat{z} \right)^2} P_3 + \frac{1}{r}\sqrt{r^2 - \hat{z}^2} P_4 = 3\frac{\sqrt{2}}{2} t + 2\frac{A_B}{r}.$$

Thus

$$\begin{aligned} \Sigma'(t) &= 3\frac{\sqrt{2}}{2} t + 2\frac{A_B}{r} + \sqrt{\frac{2}{3}} A'_T - \frac{\hat{z}}{r} A'_B \\ &= g'(t) \end{aligned}$$

as desired. Since g and Σ are continuous, and are differentiable everywhere, we may apply the Fundamental Theorem of Calculus and conclude that the surface area $\Sigma(t_1) - \Sigma(t_0)$ is $g(t_1) - g(t_0) = \frac{3\sqrt{2}}{4} s^2 + \frac{3}{r}\mathcal{V}$.

q.e.d.

References

[1] Ken Brakke. Surface evolver, version 2.30. Available at `http://www.susqu.edu/brakke/evolver/evolver.html`, 2008.

[2] Michael Hutchings. Soap bubbles and isoperimetric problems. Available at `http://math.berkeley.edu/~hutching/pub/bubbles.html`.

[3] Gary Lawlor. Metacalibrations. Preprint, 2008.

[4] Gary Lawlor and Frank Morgan. Paired calibrations applied to soap films, immiscible fluids, and surfaces or networks minimizing other norms. *Pacific Journal of Mathematics*, 166(1):55–83, 1994.

[5] Frank Morgan. *Riemannian Geometry*. A. K. Peters, 1998.

[6] Frank Morgan. Colloquium: Soap bubble clusters. *Reviews of Modern Physics*, 79(3):821, 2007.

[7] Jean E. Taylor. The structure of singularities in soap-bubble-like and soap-film-like minimal surfaces. *The Annals of Mathematics*, 103(3):489–539, 1976.